First publ. in: Histochemistry and Cell Biology 110 (1998), 1, pp. 1-8

Roland Kissmehl · Karin Hauser
Markus Gössringer · Massoud Momayezi
Norbert Klauke · Helmut Plattner

Immunolocalization of the exocytosis-sensitive phosphoprotein, PP63/parafusin, in *Paramecium* cells using antibodies against recombinant protein

Abstract We have localized a structure-bound fraction of the exocytosis-sensitive phosphoprotein, PP63/parafusin (PP63/pf), in *Paramecium* cells by widely different methods. We combined cell fractionation, western blots, as well as light and electron microscopy (pre- and post-embedding immunolabeling), applying antibodies against the recombinant protein. PP63/pf is considerably enriched in certain cortical structures, notably the outlines of regular surface fields (kinetids), docking sites of secretory organelles (trichocysts) and the membranes of subplasmalemmal Ca^{2+}-stores (alveolar sacs). From our localization studies we tentatively derive several potential functions for PP63/pf, including cell surface structuring, assembly of exocytosis sites, and/or Ca^{2+} homeostasis.

Introduction

Paramecium cells perform synchronous exocytosis of their trichocysts in response to the secretagogue, aminoethyldextran (AED; Plattner et al. 1993). Their cell membrane is largely lined with alveolar sacs, i.e. vast subplasmalemmal Ca^{2+} stores (Stelly et al. 1991, 1995; Knoll et al. 1993; Länge et al. 1995) containing a calsequestrin-like Ca^{2+}-binding protein (Plattner et al. 1997). Ca^{2+} required for exocytosis comes in part from these stores (Knoll et al. 1993; Stelly et al. 1995; Erxleben et al. 1997; Klauke and Plattner 1997).

In *Paramecium*, exocytosis is strictly paralleled by dephosphorylation of a 63 kDa phosphoprotein (PP63 → P63), which is identical with parafusin (pf; Gilligan and Satir 1982; Zieseniss and Plattner 1985), precisely within the time required for exocytosis (Höhne-Zell et al. 1992). The capacity to dephosphorylate PP63 to P63 in response to AED strictly parallels the number of extrudable trichocysts, i.e., it depends on the assembly of functional docking/fusion sites (Zieseniss and Plattner 1985). All this strongly suggests involvement of PP63/pf in exocytosis regulation. Surprisingly, PP63 or P63/pf is a phosphoglucomutase (PGM; Hauser et al. 1997).

In our attempt to discover the functional implications of PP63/pf and its exocytosis-coupled dephosphorylation, we have now performed immunolocalization studies using antibodies (ABs) against recombinant P63/pf/PGM. We show a cortical enrichment of the antigen, using widely different protocols, considering that the antigen is only loosely structure bound (Höhne-Zell et al. 1992), in accordance with hydrophobicity plots (Hauser et al. 1997).

R. Kissmehl · K. Hauser · M. Gössringer · M. Momayezi
N. Klauke · H. Plattner (✉)
Faculty of Biology, University of Konstanz, Konstanz,
PO Box 5560, D-78434 Konstanz, Germany
Tel. +49-7531-88-2228; fax +49-7531-88-2245

Materials and methods

Materials

Unicryl resin was obtained from British BioCell International (Cardiff, UK), Lowicryl K4M from Lowi (Waldkraiburg, Germany). For ABs, IgGs and conjugates, see below. For recombinant P63/pf and other materials, see Hauser et al. (1997) and Kissmehl et al. (1997).

Cell culture and cell fractionation

Paramecium tetraurelia wild-type cells, strain 7S, were grown at 25°C in sterile media to early stationary phase. Whole cell homogenates were prepared in 20 mM HEPES-HCl buffer, pH 7.0, with 0.5 M sucrose added, and centrifuged at 100 000×*g* for 60 min at 4°C. Cell surface complexes (cortices) were prepared according to Lumpert et al. (1990). For isolation of subplasmalemmal calcium stores (alveolar sacs), see Stelly et al. (1991) and Länge et al. (1995). For isolation of trichocysts (with membranes), see Glas-Albrecht and Plattner (1990); for somatic plasmalemma vesicles (i.e., non-ciliary cell membranes), see Smith and Hennessey (1993). Cilia were obtained by routine deciliation by Ca^{2+} shock. During fractionation we added a protease inhibitor cocktail consisting of 15 μM pepstatin A, 100 mU/ml aprotinin, 100 μM leupeptin, 0.26 mM TAME (Sigma, Deisenhofen, Germany), and 0.2 mM Pefabloc SC (Merck, Darmstadt, Germany).

Recombinant P63/pf, protein determination, and ABs

P63/pf cDNA was isolated from a lambda-ZAP cDNA library of *P. tetraurelia* and, after changing all codons deviating from universal genetic code into the universal codons, the cDNA was expressed in *Escherichia coli*. The recombinant protein contained a His10 tag and was purified by Ni^{2+}-affinity chromatography (Hauser et al. 1997).

Proteins were determined by the Bradford method.

Polyclonal antisera against recombinant P63/pf were raised in rabbits (strain Chbb bastard) as previously described (Hauser et al. 1997). An IgG fraction was affinity-purified by ammonium sulfate precipitation, followed by affinity chromatography on recombinant P63/pf coupled to activated CH Sepharose 4B (Pharmacia LKB Biotechnology, Freiburg, Germany).

ELISA, slot blots, electrophoresis, and western blots

ABs against recombinant P63/pf were characterized by ELISA as described (Momayezi et al. 1996). For slot blots, see Kissmehl et al. (1997). For electrophoresis, samples were denatured by boiling for 3 min in sample buffer (0.4 M TRIS-HCl, 1% SDS, 0.5% dithiothreitol, 20% glycerol, pH 8.0), subjected to electrophoresis in linear gradient (5–10% or 5–15%) SDS polyacrylamide gels, and processed for western blots as outlined by Momayezi et al. (1996) and Kissmehl et al. (1997), using alkaline phosphatase-coupled second ABs.

OD readings in ELISA and reaction intensities on western blots obtained by the AB reaction (*a*) were referred, for the different samples, to the amounts of protein applied (*b*). These values were calibrated by normalizing to similar *a/b* values obtained with the original P63/pf. On this basis, we calculated the subcellular distribution of P63/pf in Table 1. We ascertained that all readings of reaction intensities were within the linear range. Densitometric quantification was performed using the Bio-1d analysis software for electrophoresis images provided for the Vilber Lourmat Biotechnology densitometer by the same company (Marne La Vallée, France; Fröbel, Lindau, Germany).

Immunolocalization

Pretreatments for preembedding and fluorescence labeling

Cells were washed twice in 10 mM PIPES-HCl buffer pH 7.2 (10 mM $MgCl_2$, 0.1 mM $CaCl_2$) before fixation (a) for 15 min at room temperature (RT) in 4% w/v formaldehyde, dissolved in phosphate-buffered saline (PBS, 0.2 M, pH 7.2), containing 0.05% v/v Triton X-100, 1% saponin or 0.02% digitonin as permeabilizing agents (with the same results); or (b) for 10 min in equal parts of methanol and acetone on ice, followed by 4% formaldehyde for 15 min. All samples were washed 3×10 min each in PBS containing 50 mM glycine.

Immunofluorescence labeling

Cells fixed by method (b) were incubated at RT with affinity-purified rabbit anti-P63/pf ABs (0.375 mg/ml, diluted 1:30) for up to 90 min. Samples were washed 3 times in PBS and incubated with fluorescein-conjugated goat anti-rabbit IgGs (BioTrend Chemikalien, Köln, Germany) for 60 min. After rinsing with PBS, samples were analyzed in a Zeiss photomicroscope with BP485, FT510, and LP520 filters, and, in parallel, in a confocal laser scanning microscope (CLSM), type Odyssey-LSM-C, from Noran (Bruchsal, Germany), combined with a Zeiß Axiovert microscope and a 100-mW Ar laser, using 488-nm excitation and 515-nm emission wavelengths.

Postembedding immunogold labeling

Cells were fixed at 4°C for 30 min: (a) in 4% formaldehyde; or (b) in 4% formaldehyde plus 0.25% glutaraldehyde, both in PBS, washed and dehydrated in increasing ethanol concentrations (30, 50, 70, 80, and 2×100%), impregnated with Unicryl resin at 0°C (2 h and then overnight), and polymerized at –25°C by UV irradiation (two lamps at 15 W, 3 days). Method (b) was also combined with progressive lowering temperature dehydration and embedding in Lowicryl K4 M (UV polymerization at –30°C).

Ultrathin sections collected on Formvar-coated nickel grids were pretreated for 2×10 min on 20 µl droplets of PBS pH 7.4 and 2×15 min on 0.2% BSA-c (BioTrend) in PBS. Then, grids were placed on drops of 0.2% BSA-c/PBS with primary ABs for 60 min at RT or overnight at 4°C. Grids were washed in BSA-c/PBS (3×10 min) and, also at RT, incubated for 1 h with 6-nm goldlabeled goat anti-rabbit IgGs or protein A. Gold-labeled sections for electron microscopy (EM) were rinsed in distilled water, fixed with 1% glutaraldehyde (5 min), and routinely stained. Postembedding Au-labeled EM sections [fixation (b)] were used for quantitation. Gold label was referred to the size of the structures evaluated and this was determined by the hit point method (see Plattner and Zingsheim 1983).

Controls and additional labeling experiments

Preembedding experiments (with permeabilized cells) were done to serve as a link between CLSM analysis (requiring permeabilized cells) and postembedding labeling at the EM level (without permeabilization hazards). In preembedding immunogold labeling experiments, fixed and permeabilized cells [see method (b), above, under Pretreatments] were incubated with primary ABs and incubated (≤ 90 min, RT) with goat anti-rabbit IgGs or with protein A, both conjugated to 6-nm gold particles (BioTrend). After three washes in PBS cells were postfixed with 2.5% v/v glutaraldehyde in cacodylate buffer (0.1 M, pH 7.1) for 10 min at RT, washed twice and exposed to 1% w/v OsO_4, also in cacodylate buffer, for 45 min. Then, samples were processed as described previously (Momayezi et al. 1996). Samples were dehydrated in a graded acetone series and embedded in Spurr's resin. For controls, anti-P63/pf ABs were preadsorbed with an excess of recombinant P63/pf, or normal preimmune serum was substituted for primary ABs. We also used peroxidase (POX)-tagged second ABs at light microscopy (LM) and EM levels (Momayezi et al. 1996).

Results

ABs, cell fractionation, and western blot analysis

Affinity-purified ABs used had previously been shown on western blots to recognize PGM from chicken or rabbit muscle, recombinant P63/pf, and the corresponding protein, P63/pf/PGM, in *Paramecium* cells (Hauser et al. 1997). Reactivity is abolished after preadsorption with an excess of recombinant antigen, as we confirm.

Figure 1 shows the P63/pf distribution in subcellular fractions from *Paramecium* on western blots (5–15% gels). Reactivity detected in the whole cell homogenate is largely recovered in the 100 000 *g* supernatant, but only variable, small amounts in the pellet. (For statistical evaluation of western and slot blots, see Table 1.) This reflects the solubility of the antigen, while its partial retention in isolated cortex fragments reflects the presence of a substantial structure-bound fraction. Why the antigen consistently exhibits a slightly higher apparent molecular mass when contained in the cortex (Fig. 1, lane 4), equiv-

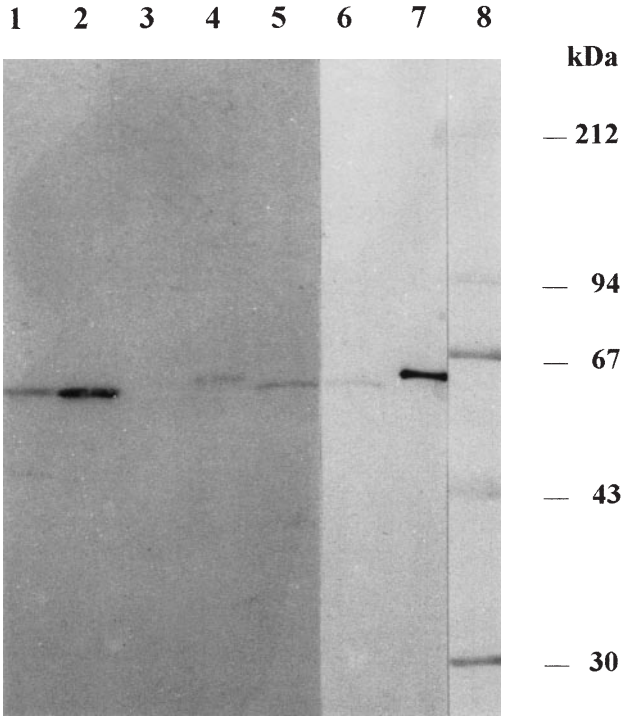

Fig. 1 Western blot analysis of the subcellular distribution of P63/parafusin (pf) using affinity-purified antibodies (ABs); 5–15% gradient gels. Aliquots of either 50 µg protein of whole cell homogenates (*lane 1*), 100 000 *g* supernatant (*lane 2*), 100 000×*g* pellet (*lane 3*), isolated cortices (*lane 4*), cilia (*lane 5*), somatic plasmalemma vesicles (*lane 6*) or, as a reference, 50 ng of recombinant P63/pf (*lane 7*) were applied. *Lane 8* contains standard proteins. Note strong immunoreactivity in the 100 000 *g* supernatant (*lane 2*) reflecting the solubility of the majority of P63/pf, while a minor proportion remains structure-bound (*lanes 4–6*)

Table 1 Subcellular distribution of P63/parafusin (pf) derived from cell fractionation and antibody (AB) binding analyses. From relative protein contents and from concentrations of P63/pf determined by AB binding in slot blots and western blots (values normalized to standard samples of recombinant P63/pf and to equal protein concentrations), relative P63/pf contents were calculated as a percentage of the total protein in a sample. From these values, the distribution of P63/pf in the cell and the relative concentrations have been calculated. Values ±SD

Sample	Relative protein content[a] (%), *n*	Relative P63/pf content (%), *n*	Distribution of P63/pf[a] (%)	Relative concentration of P63/pf
Homogenate	100	0.095, 7	100	1.00
100 000 *g* supernatant	48.0±6.2, 5	0.180, 4	90.4	3.95
Cortices	15.2±12.4, 3	0.015, 7	2.4	1.05
Alveolar sacs	0.5±0.1, 3	0.130, 3	0.7	273.70

[a] Values do not add up to 100% because there is no complete fractionation schedule available for our cells

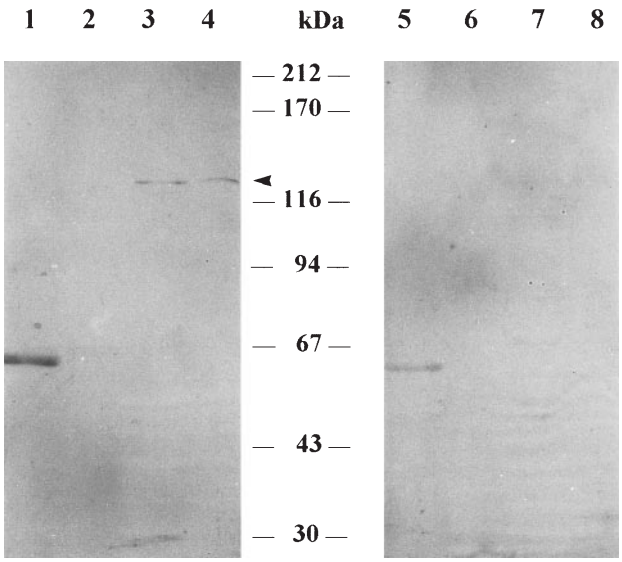

Fig. 2 Western blot analysis of subcellular compartments involved in exocytosis or in Ca^{2+} mobilization; 5–10% gradient gels. Affinity-purified IgGs against recombinant P63/pf were applied before (*lanes 1–4*) or after preadsorption with the antigen (*lanes 5–8*). For immunobinding analysis, we used 50 µg protein from the 100 000 *g* supernatant (*lanes 1, 5*), 100 000 *g* pellets (*lanes 2, 6*), isolated cortices (*lanes 3, 7*) or alveolar sacs (*lanes 4, 8*). Note immuno-reactive bands in isolated cortices (*lane 3*) and in alveolar sacs (*lane 4*) at ca. 128 kDa (*arrowhead*), which are abolished when ABs are preincubated with recombinant P63/pf at a molar ratio of 1:5 (*lanes 7, 8*). This may reflect dimerization of structure-bound P63/pf. In the supernatant, preadsorption of ABs does significantly reduce, though not entirely block, immunodetection (cf. *lanes 1, 5*) because of the molar ratio used. The lack of immunobinding in the particulate fraction of whole cell homogenates (*lane 2* in Fig. 2 and *lane 3* in Fig. 1) reflects the reduced content of P63/pf in these fractions

alent to that of the poly-His-tagged recombinant form (Fig. 1, lane 7), has not yet been analyzed in any detail. Among cortical structures, somatic cell membrane vesicles (and cilia) were reactive, while isolated trichocysts were not (not shown). This is compatible with our structural localization studies (see below). This also holds for P63/pf in isolated alveolar sacs. A dimeric (126 kDa) form of the antigen can be seen in alveolar sacs or cortices on some of the western blots (5–10% gels, Fig. 2). The occurrence of a monomer and/or dimer form corresponds to data reported in the biochemical literature for PGM (Lin et al. 1986; Dai et al. 1992). In neither that case (PGM), nor in our case (P63/pf) have the critical parameters been determined which might govern monomer/dimer transition. Although either form might occur under quite similar conditions when P63/pf is analyzed in a structure-bound form (cf. Figs. 1, 2), in agreement with the crystallographic data reported for PGM, only the monomeric form was detected in supernatant extracts.

In Table 1, immunological data are normalized to recombinant P63/pf as a standard, and, taking into account the protein content per sample, we calculated the relative contents and concentrations of P63/pf in our fractions (for details, see Materials and methods). Thus, P63/pf represents 0.095% of the total cell protein. It contributes only 0.015% to cortical protein content, although 2.4% of cellular P63/pf occurs there. Since cortices, in addition to alveolar sacs and ciliary bases, contain docked trichocysts with vast masses of secretory proteins (Vilmart-Seuwen et al. 1986), it is not surprising that the

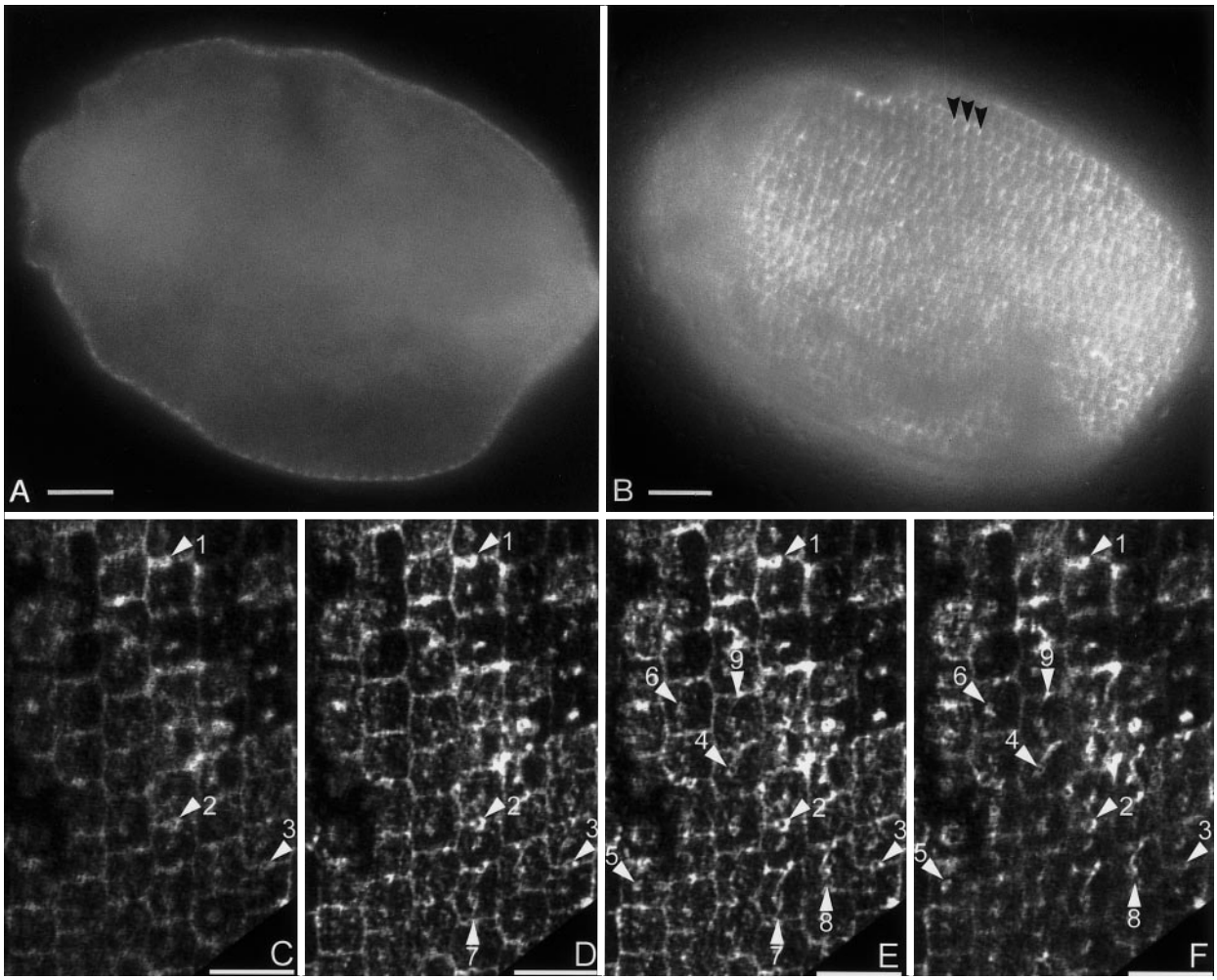

Fig. 3A–F Immuno-FITC localization of P63/pf. Cells processed for light microscopy, method (b), were incubated with affinity-purified anti-P63/pf IgGs, followed by FITC-coupled goat anti-rabbit IgGs. **A** Median, **B** superficial focus planes in conventional fluorescence. Note selective cortical labeling (**A**), outlining surface fields (kinetids) in **B** with bright dots (trichocyst docking sites) in the middle of perpendicular ridges of the cell surface (*arrowheads*). **C–F** Confocal laser scanning micrographs from the cell surface in 0.6-μm z-steps. Note outlines of kinetids with longitudinal (vertical) and perpendicular ridges, the latter with dot- or ring-like labeling in the center (docking site proper and collar of docked trichocysts, *arrowheads* 1–3). Also note ciliary bases in the center of kinetids (*arrowheads 4–6*) and borders of adjacent alveolar sacs along the vertical center line of some kinetids (*arrowheads 7–9*). *Bars* **A, B** 10 μm, C–F 5 μm

P63/pf concentration in cortex fractions is only a little above average. This underscores the value of structural analyses (see below) in demonstrating not only enrichment of P63/pf on alveolar sacs, as indicated in Table 1, but also on some other cortical structures.

LM localization studies

Immunofluorescence analysis of permeabilized cells reveals antigen confinement to the cell cortex (Fig. 3A, B; conventional fluorescence). Since fixation and permeabilization were performed simultaneously, this may explain why the immunofluorescence is intense relative to the mediocre staining of immunoreactive bands on western blots. The following identification of labeled structures is based on knowledge of their regular arrangement in a *Paramecium* cell (see Plattner et al. 1993) and on EM labeling experiments: (a) by the preembedding procedures described in Materials and methods (data not shown) using similar pretreatments to those required for fluorescence labeling; and (b) by postembedding methods which are largely devoid of the hazard of antigen redistribution (see data below). All data are compatible. The occurrence of a firmly structure-bound fraction of P63/pf reflects data obtained with western blots from subcellular fractions (see above).

Figure 3 (C–F) documents staining, viewed in a CLSM, of the outlines of the regularly arranged surface fields (kinetids), characteristic of *Paramecium* cells, as well as of dots in their center (ciliary bases) and of dot- or ring-like structures on many of the perpendicular ridges of individual fields (docking sites of trichocysts). In CLSM analysis using discrete z-steps, these hollow structures have a length corresponding to the collar, i.e., proteins attached to docked trichocysts (Plattner et al.

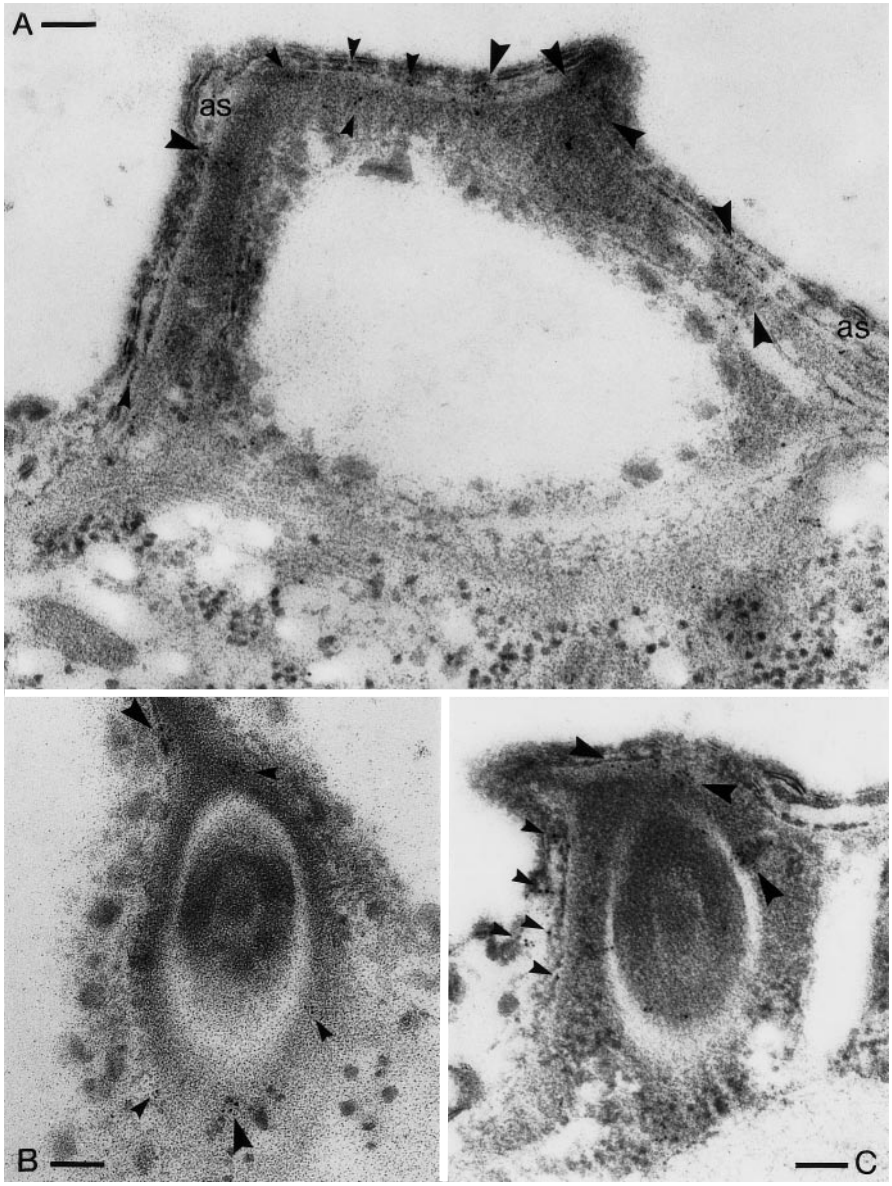

Fig. 4A–C Immunogold localization of P63/pf by postembedding (non-permeabilized cells), using anti-P63/pf ABs, followed by goat anti-rabbit IgG-6-nm colloidal gold and slight glutaraldehyde postfixation. **A** *Arrowheads* of different size indicate different intensities of labeling concentrated over the inner boundary of alveolar sacs (*as*), or materials closely associated with it, cut in a tangential plane. *B*, *C* Trichocyst tips cut at a lower (**B**) or upper (**C**) position relative to the cell membrane, representing the docking site proper. Note labeling of materials associated with trichocyst tips, as indicated by larger or smaller *arrowheads*, respectively. *Bars* 0.1 μm

1993). Alveolar sac rims are also stained as faint longitudinal lines along the center line of some kinetids (Fig. 3E). They follow the longitudinal axes formed by ciliary bases and trichocyst docking sites, as indicated by arrowheads in Fig. 3 (C–F).

Other labeling studies and controls

To establish a link with ultrastructural analyses, POX labeling was investigated at the LM and EM levels (not shown), the latter also including preembedding labeling with colloidal gold techniques. Again, the cell cortex was selectively labeled, particularly along alveolar sacs and on trichocyst docking sites (for EM analysis, see below). Again, preadsorption of primary ABs with the original antigen or substitution by preimmune serum abolished labeling in LM and EM analyses (not shown).

EM localization studies

POX-coupled second ABs yield reaction product on trichocyst docking sites and along alveolar sac membranes, with frequent concentration on the inner part facing the cell center (not shown). P63/pf localization has been analyzed in more detail by gold labeling according to the pre- (not shown) or post-embedding method (Fig. 4). In both cases, labeled structures again encompass trichocyst attachment sites and some parts of alveolar sac membranes, particularly the inner part close to trichocysts and to ciliary bases. Both postembedding procedures used, after fixation method (b) as outlined in Materials and methods, gave equal results. In Fig. 4, labeling of inner alveolar sac membranes and/or possibly of attached cytoplasmic materials becomes particularly evident on grazing sections (Fig. 4A). According to quantitation in Table 2, the outer alveolar membrane-

Table 2 Relative labeling density of subcellular structures by anti-P63/pf/phosphoglucomutase ABs, followed by gold-coupled protein A-gold (postembedding method). Gold grains were collected from seven different cell sections and normalized to the area determined for a given structure determined by the hit point method. Off-cell background was subtracted and labeling density (Au/μm²) was normalized to that over the cytoplasm (=1.00) as a reference. (*n* Number of structures analyzed)

Structure analyzed	Relative labeling density	*n*
Cytoplasm[a]	1.00	6
Nucleus	0.40	3
Mitochondria	0.45	4
Surface ridges	2.00*	4
Collar	55.30*	3
Trichocyst contents[b]		
Tip	0.20	7
Body	0.00	4
Alveolar sacs+attached materials[c]	24.60*	6

* Significantly above general cytoplasmic labeling ($P \leq 0.01$)

[a] Cell regions devoid of the organelles which are specifically mentioned in the table and which were evaluated separately

[b] Trichocysts are composed of a tip (for docking at the cell membrane) and a crystalline body (=matrix, the main portion of secretory proteins), both being wrapped by a common membrane

[c] Both inner and outer alveolar membranes, i.e., that facing the cell interior and that closely apposed to the cell membrane, were labeled. No distinction was made between the two faces, the alveolar membranes proper and attached epiplasm (on the inner alveolar membrane) or the subplasmalemmal space and cell membrane (on the outer alveolar membrane). These structures were analyzed as a complex, since discrimination was not possible in our evaluations

plasmalemma complex is also labeled. Most remarkably, trichocyst docking sites are labeled (Fig. 4B, C), notably the protein material surrounding trichocyst tips (collar). This corresponds to LM data (Fig. 3), which also shows labeling of the trichcoyst attachment site proper.

Quantitation of gold labeling in Table 2 is in line with and complements data from cell fractionation and LM labeling (see above). The latter would tend to underestimate intense labeling of small, delicate structures. As in immunochemical analyses, the major fraction of the cytoplasm contains abundant P63/pf/PGM, while many organelles are not significantly labeled (Table 2).

Discussion

We can clearly localize in *Paramecium* cells a significant structure-bound fraction of P63/pf to cortical structures, including alveolar sacs (particularly their inner part) and trichocyst docking sites. The protein which we have localized may, therefore, possibly not be related to glycogen turnover, rather, it may represent one of the PGM forms which are enzymatically inactive in vivo, as known from other systems (see below).

What might be the functional implications of our findings? Could, nevertheless, aspects of energy supply during exocytosis play a role, e.g., in the context of Ca^{2+} signaling and re-establishment of Ca^{2+} homeostasis (Klauke and Plattner 1997)? A priori, this would appear possible, since such a function has been discussed for PGM associated with sarcoplasmic reticulum (SR) in muscle cells (Han et al. 1992; Cuenda et al. 1993; Nogues et al. 1996) and since alveolar sacs in some respects resemble SR (Länge et al. 1995; Erxleben et al. 1997; Plattner et al. 1997). However, ATP hydrolysis lags far behind synchronous AED-induced exocytosis (Vilmart-Seuwen et al. 1986) and PP63 dephosphorylation (Höhne-Zell et al. 1992). This and the lack of glycogen-like particles in P63/pf-labeled zones make any role in ATP supply questionable, although not impossible.

For the SR, some other functional aspects have been discussed, not only for PGM (Lee et al. 1992; Coronado et al. 1994) but also for some other glycolytic enzymes (Fothergill-Gilmore and Michels 1993). Among such possiblities is the association with Ca^{2+} stores, specifically with their Ca^{2+}-release channels. In this case, PGM and some downstream glycolytic enzymes may function as modulatory proteins bound to Ca^{2+}-release channels (Corbett et al. 1985; Rios and Pizarro 1991; Lee et al. 1992; Coronado et al. 1994; Sutko and Airey 1996). PGM is also associated with microsomal membranes from other cell types (Mithieux et al. 1995). For PGM a regulatory function in Ca^{2+} release from SR is known to depend on the phosphorylation state and to be independent of enzymatic activity which is reversibly lost by structure binding (Lee et al. 1992). In fact, there is evidence that alveolar sacs contribute Ca^{2+} to AED-stimulated exocytosis (Knoll et al. 1993; Stelly et al. 1995; Erxleben et al. 1997). In this context, it may turn out functionally important in future analyses that P63/pf can form dimers in structure-bound form (this paper), just as PGM does after crystallization (Lin et al 1986, Dai et al. 1992), while dimers, as we have shown, are not maintained in solution.

There is a bewildering variety of other functional aspects suggested for glycolytic enzymes, mainly on the basis of gene sharing involving different functions for one and the same protein (Piatigorsky and Wistow 1989; Smalheiser 1996). This also includes structure formation, e.g., formation of lens crystallin (Piatigorsky and Wistow 1989; Wistow 1993) or association with cytoskeletal elements (Frederici et al. 1996). In muscle, PGM can associate with desmosomes (Belkin et al. 1994), extra-junctional acetylcholine receptors (Belkin and Burridge 1994) or dystrophin (Moiseeva et al. 1996). Functional diversity has been inferred in mammals from the genetic variability of PGM (Putt et al. 1993). Similarly, we have found two P63/pf genes (Hauser et al. 1997). Association of P63/pf with protein-rich cortical structures would be compatible with such a role.

In the *Paramecium* cortex, P63/pf exhibits a distribution pattern similar, in part, to that of calmodulin (Momayezi et al. 1986; Kerboeuf et al. 1993). While association of both proteins has not been analyzed in detail, it is interesting to note that P63/pf is dephosphorylated in vitro by a Ca^{2+}-calmodulin-activated phosphatase type 2B (Kissmehl et al. 1997). In other systems, PGM is report-

ed to associate with the cytosolic Ca^{2+}-binding protein, S100 (Landar et al. 1996).

In conclusion, our finding of a cortical localization of P63/pf is compatible with a role in rapid signal transmission during stimulus-secretion coupling in *Paramecium* cells. The protein might also be involved, for example, in an enzymatically inactive form, in the assembly of components relevant for structuring the cell cortex, secretory organelle docking, and/or membrane fusion processes, and/or Ca^{2+} signaling, as discussed for muscle cells. While we could pinpoint structural targets of P63/pf function, any further functional analysis will be facilitated by the availability of mutants (see Introduction).

Acknowledgements We thank Ms S. Kolassa and B. Kottwitz for excellent technical assistance. Supported by the Deutsche Forschungsgemeinschaft, grants SFB156/B4 and Forschergruppe "Struktur und Funktionssteuerung an zellulären Oberflächen" project P4.

References

Belkin AM, Burridge K (1994) Expression and localization of the phosphoglucomutase-related cytoskeletal protein, aciculin, in skeletal muscle. J Cell Sci 107:1993–2003

Belkin AM, Klimanskaya IV, Lukashev ME, Lilley K, Critchley DR, Koteleliansky VE (1994) A novel phosphoglucomutase-related protein is concentrated in adherens junctions of muscle and nonmuscle cells. J Cell Sci 107:159–173

Corbett AM, Caswell AH, Brandt NR, Brunschwig JP (1985) Determinants of triad junction reformation: identification and isolation of an endogenous promoter for junction reformation in skeletal muscle. J Membr Biol 86:267–276

Coronado R, Morrissette J, Sukhareva M, Vaughan DM (1994) Structure and function of ryanodine receptors. Am J Physiol 266:C1485-C1504

Cuenda A, Nogues M, Gutiérrez-Merino C, DeMeis L (1993) Glycogen phosphorolysis can form a metabolic shuttle to support Ca^{2+} uptake by sarcoplasmic reticulum membranes in skeletal muscle. Biochem Biophys Res Commun 196:1127–1132

Dai JB, Liu Y, Ray WJ, Konno M (1992) The crystal structure of muscle phosphoglucomutase refined at 2.7 Angstrom resolution. J Biol Chem 267:6322–6337

Erxleben C, Klauke N, Flötenmeyer M, Blanchard MP, Braun C, Plattner H (1997) Microdomain Ca^{2+} activation during exocytosis in *Paramecium* cells. Superposition of local subplasmalemmal calcium store activation by local Ca^{2+} influx. J Cell Biol 136:597–607

Fothergill-Gilmore LA, Michels PAM (1993) Evolution of glycolysis. Progr Biophys Mol Biol 59:105–235

Frederici C, Camoin L, Hattab M, Strosberg AD, Couraud PO (1996) Association of the cytoplasmic domain of intercellular adhesion molecule-1 with glyceraldehyde-3-phosphate dehydrogenase and β-tubulin. Eur J Biochem 238:173–180

Gilligan DM, Satir BH (1982) Protein phosphorylation/dephosphorylation and stimulus-secretion coupling in wild type and mutant *Paramecium*. J Biol Chem 257:13903–13906

Glas-Albrecht R, Plattner H (1990) High yield isolation procedure for intact secretory organelles (trichocysts) from *Paramecium tetraurelia* strains. Eur J Cell Biol 53:164–172

Han JW, Thieleczek R, Varsányi M, Heilmeyer LMG (1992) Compartmentalized ATP synthesis in skeletal muscle triads. Biochemistry 31:377–384

Hauser K, Kissmehl R, Linder J, Schultz JE, Lottspeich F, Plattner H (1997) Identification of isoforms of the exocytosis-sensitive phosphoprotein PP63/parafusin in *Paramecium tetraurelia* and demonstration of phosphoglucomutase activity. Biochem J 323:289–296

Höhne-Zell B, Knoll G, Riedel-Gras U, Hofer W, Plattner H (1992) A cortical phosphoprotein ('PP63') sensitive to exocytosis triggering in *Paramecium* cells. Biochem J 286:843–849

Kerboeuf D, LeBerre A, Dedieu JC, Cohen J (1993) Calmodulin is essential for assembling links necessary for exocytotic membrane fusion in *Paramecium*. EMBO J 12:3385–3390

Kissmehl R, Treptau T, Kottwitz B, Plattner H (1997) Occurrence of a *para*-nitrophenyl phosphate phosphatase with calcineurin-like characteristics in *Paramecium tetraurelia*. Arch Biochem Biophys 344:260–270

Klauke N, Plattner H (1997) Imaging of Ca^{2+} transients induced in *Paramecium* cells by a polyamine secretagogue. J Cell Sci 110:975–983

Knoll G, Grässle A, Braun C, Probst W, Höhne-Zell B, Plattner H (1993) A calcium influx is neither strictly associated with nor necessary for exocytotic membrane fusion in *Paramecium* cells. Cell Calcium 14:189–199

Landar A, Caddell G, Chessher J, Zimmer DB (1996) Identification of an S100A1/S100B target protein: phosphoglucomutase. Cell Calcium 20:279–285

Länge S, Klauke N, Plattner H (1995) Subplasmalemmal Ca^{2+} stores of probable relevance for exocytosis in *Paramecium*. Alveolar sacs share some but not all characteristics with sarcoplasmic reticulum. Cell Calcium 17:335–344

Lee YS, Marks AR, Gureckas N, Lacro R, Nadal-Ginard B, Kim DH (1992) Purification, characterization, and molecular cloning of a 60-kDa phosphoprotein in rabbit skeletal sarcoplasmic reticulum which is an isoform of phosphoglucomutase. J Biol Chem 267:21080–21088

Lin ZJ, Konno M, Abad-Zapatero C, Wierenga R, Murthy MRN, Ray WJ, Rossmann MG (1986) The structure of rabbit muscle phosphoglucomutase at intermediate resolution. J Biol Chem 261:264–274

Lumpert CJ, Kersken H, Plattner H (1990) Cell surface complexes ('cortices') isolated from *Paramecium tetraurelia* cells as a model system for analysing exocytosis in vitro in conjunction with microinjection studies. Biochem J 269:639–645

Mithieux G, Ajzannay A, Minassian C (1995) Identification of membrane-bound phosphoglucomutase and glucose-6 phosphatase by ^{32}P-labeling of rat liver microsomal membrane proteins with ^{32}P-glucose-6 phosphate. J Biochem (Tokyo) 117:908–914

Moiseeva EP, Belkin AM, Spurr NK, Koteliansky VE, Critcheley DR (1996) A novel dystrophin/utrophin-associated protein is an enzymatically inactive member of the phosphoglucomutase superfamily. Eur J Biochem 235:103–113

Momayezi M, Kersken H, Gras U, Vilmart-Seuwen J, Plattner H (1986) Calmodulin in *Paramecium tetraurelia*: localization from the in vivo to the ultrastructural level. J Histochem Cytochem 34:1621–1638

Momayezi M, Wloga D, Kissmehl R, Plattner H, Jung G, Klumpp S, Schultz JE (1996) Immunolocalization of protein phosphatase type 1 in *Paramecium* cells using antibodies against recombinant protein and peptides. J Histochem Cytochem 44:891–905

Nogues M, Cuenda A, Henao F, Gutiérrez-Merino C (1996) Ca^{2+} uptake coupled to glycogen phosphorolysis in the glycogenolytic-sarcoplasmic reticulum complex from rat skeletal muscle. Z Naturforsch 51c:591–598

Piatigorsky J, Wistow GJ (1989) Enzyme/crystallins: gene sharing as an evolutionary strategy. Cell 57:197–199

Plattner H, Zingsheim HP (1983) Electron microscopic methods in cellular and molecular biology. Subcell Biochem 9:1–236

Plattner H, Knoll G, Pape R (1993) Synchronization of different steps of the secretory cycle in *Paramecium tetraurelia*: trichocyst exocytosis, exocytosis-coupled endocytosis, and intracellular transport. In: Plattner H (ed) Membrane traffic in protozoa. JAI Press, Greenwich (CT), London, pp 123–148

Plattner H, Habermann A, Kissmehl R, Klauke N, Majoul I, Söling HD (1997) Differential distribution of calcium stores in *Paramecium* cells. Occurrence of a subplasmalemmal store with a calsequestrin-like protein. Eur J Cell Biol 72:297–306

Putt W, Ives JH, Hollyoake M, Hopkinson DA, Whitehouse DB, Edwards YH (1993) Phosphoglucomutase 1: a gene with two promoters and a duplicated first exon. Biochem J 296:417–422

Rios E, Pizarro G (1991) Voltage sensor of excitation-contraction coupling in skeletal muscle. Physiol Rev 71:849–908

Smalheiser NR (1996) Proteins in unexpected locations. Mol Biol Cell 7:1003–1014

Smith TM, Hennessey TM (1993) Body plasma membrane vesicles from *Paramecium* contain a vanadate-sensitive Ca^{2+}-ATPase. Anal Biochem 210:299–308

Stelly N, Mauger JP, Kéryer G, Claret M, Adoutte A (1991) Cortical alveoli of *Paramecium*: a vast submembranous calcium storage compartment. J Cell Biol 113:103–112

Stelly N, Halpern S, Nicolas G, Fragu P, Adoutte A (1995) Direct visualization of a vast cortical calcium compartment in *Paramecium* by secondary ion mass spectrometry (SIMS) microscpy: possible involvement in exocytosis. J Cell Sci 108:1895–1909

Sutko JL, Airey JA (1996) Ryanodine receptor Ca^{2+} release channels: does diversity in form equal diversity in function? Physiol Rev 76:1027–1071

Vilmart-Seuwen J, Kersken H, Stürzl R, Plattner H (1986) ATP keeps exocytosis sites in a primed state but is not required for membrane fusion: an analysis with *Paramecium* cells in vivo and in vitro. J Cell Biol 103:1279–1288

Wistow G (1993) Lens crystallins: gene recruitment and evolutionary dynamism. Trends Biochem Sci 18:301–306

Zieseniss E, Plattner H (1985) Synchronous exocytosis in *Paramecium* cells involves very rapid (≤1 s), reversible dephosphorylation of a 65-kD phosphoprotein in exocytosis-competent strains. J Cell Biol 101:2028–2035